

*Supporting Information*

**Reverse adhesion of a gecko-inspired synthetic adhesive  
switched by ion exchange polymer metal composite actuator**

*Dong-Jie Guo<sup>a</sup>, Rui Liu<sup>a</sup>, Yu Cheng<sup>a</sup>, Hao Zhang<sup>b</sup>, Li-Ming Zhou<sup>a</sup>, Shao-Ming Fang<sup>\*a</sup>,  
Winston Howard Elliott<sup>c</sup>, Wei Tan<sup>\*c</sup>*

<sup>a</sup> State Laboratory of Surface & Interface, Zhengzhou University of Light  
Industry, Zhengzhou, China, 450002

<sup>b</sup>Institute of Bio-inspired Structure and Surface Engineering, Nanjing University  
of Aeronautics and Astronautics, Nanjing, China, 210016

<sup>c</sup>Department of Mechanical Engineering, University of Colorado, Boulder,  
USA, 80309

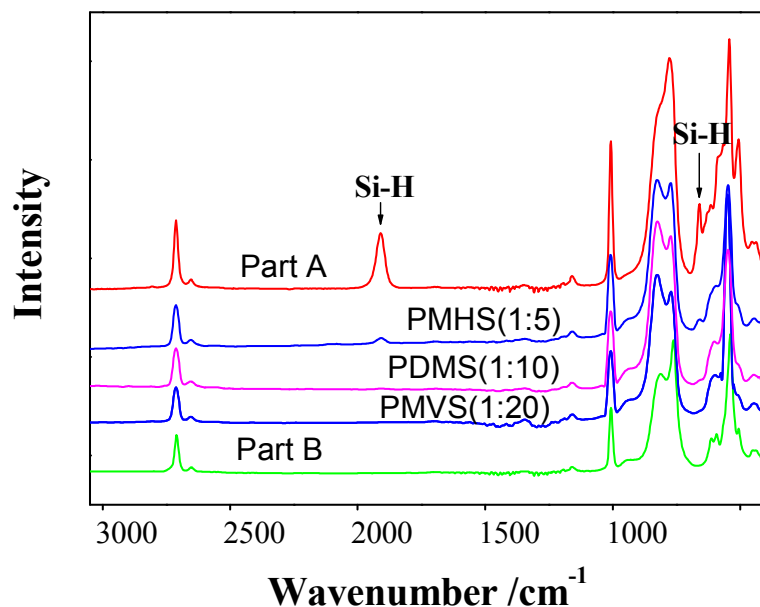
\* Corresponding Author, Correspondence should be sent to: [mingfang@zzuli.edu.cn](mailto:mingfang@zzuli.edu.cn) or  
[wtan@Colorado.Edu](mailto:wtan@Colorado.Edu)

## **S1. Preparations of PMVS and PMHS precursors**

Sylgard 186 (Midland, MI) is made of part A and part B: part A is polymethylhydrosiloxane (PMHS), whose reactive function group is Si-H, while the main content of part B is polymethylvinylsiloxane (PMVS), whose active function group is C=C. It is normally used at a weight ratio of 1:10 (A:B). At that ratio, the two functional groups of Si-H and vinylene have equal moles and the cross-linking reaction can be completely finished by vulcanization.<sup>1</sup> When the ratio is less than 1:10, such as 1:20, more vinyl groups will be present in the mixture, and after vulcanization, excess vinyl groups remain in the elastomer. On the other hand, with a ratio of 1:5, Si-H remains.

To prepare the PMVS, PDMS, and PMHS precursors, Part A and B were mixed with a ratio of 1:20, 1:10, or 1:5, and degassed under vacuum until no visible bubble was observed. Then, they were cast on plastic discs and instantly put inside a vacuum oven vulcanizing at 80 °C for 60 min before taken out for measurements with attenuated total reflectance infrared spectroscopy (ATR-IR). The IR spectra of colloid part A and B were recorded as liquid films by spreading the liquid gel on the crystal surface, respectively. As shown in S-Figure 1, the strong twin bands in the range of 1000 and 1100  $\text{cm}^{-1}$  are due to the asymmetric stretching of Si-O-Si. In the spectra of A or B, the peak at 1030  $\text{cm}^{-1}$  is stronger than that at 1072  $\text{cm}^{-1}$ , probably due to their liquid states. The two vibrations, at 2160 and 912  $\text{cm}^{-1}$ , are conventionally attributed to the

characteristic stretching and bending modes of Si-H, respectively. For PMVS, the Si-H disappeared completely due to the superfluous C=C.



**s-Figure 1.** ATR-FTIR spectra for part A, B, PMHS, PDMS, and PMVS elastomers

## S2. Synthesis of GO/Ag NPs

The graphene oxide (GO) was prepared from NFG by a modified Hummers method.<sup>2-3</sup> Briefly, NFG powder (2.0 g) was added into the mixture containing concentrated NaNO<sub>3</sub> (1.0 g) and frozen concentrated H<sub>2</sub>SO<sub>4</sub> (92 mL). KMnO<sub>4</sub> (9.0 g) was gradually added into the flask under stirring, and the mixture remained agitated for additional 24 h. To avoid any unexpected reactions, the temperature was carefully controlled to less than 4 °C by using ice water. Then, taken from the ice bath, the mixture's temperature was allowed to rise to 98 °C within 90 min. Subsequently,

deionized water (92 mL) was added into the mixture drop by drop. Finally, 10 ml of  $\text{H}_2\text{O}_2$  (40%) solution was gradually added to reduce  $\text{KMnO}_4$  residual until the solution turned to bright yellow. Deionized water (180 ml) was again added to dilute the mixture, and stirred for around 20 min to obtain a graphite oxide suspension. The mixture was centrifuged at 5000 rpm for 5 min, and then the resulting GO of the centrifugation was carefully washed by HCl solution (10%), and dialysed in deionized water to completely remove metal ions and acids. GO (200 mg) was dispersed in 200 mL of deionized water by ultrasonication for 2h, thus resulted in an exfoliated GO (1.0 mg/mL) solution.

Ammonia solution (30 %) was added into 20 mL  $\text{AgNO}_3$  (0.05 mol/L) aqueous solution drop by drop, until obtained a clear ammoniacal silver solution. Subsequently, the prepared GO solutions (200 mL) were added, and the mixture was incubated at 50 °C for 30 min. Then, 40 mL glucose solution (0.03 Mol/L) was added under violent stir for 2 min, and the mixture was incubated at 50 °C for 1 h again. The mixture was dialysed in abundant deionized water, and was centrifuged at 2000 rpm for 5 min, GO carried Ag nano particles (GO/Ag NPs) of around 0.27g were finally obtained. GO and GO/Ag NPs were put on a copper micro-grid for HRTEM (JEM-2100) observation.

### **S3. Fabrication of GO/Ag NPs doped Nafion membrane**

5.0 mL of Nafion (20%) solution was poured into a PDMS-based container with dimensions of 30 mm×40 mm×50 mm. Then, the above prepared GO/Ag NPs (0.05 g) were added, and the mixture was continually stirred until a homogeneous brown solution was obtained. This container including the inner mixture was placed into an oven for 20 hours' evaporation at 90°C, and annealed at 150°C for 5min. As a result, a brownish black hybrid membrane of GO/Ag NPs doped Nafion membrane with a thickness of around 216 μm was obtained. As a control, a pure self-casting Nafion membrane without adding GO/Ag NPs was also prepared with the same Nafion content, yielding a thickness of around 192 μm.

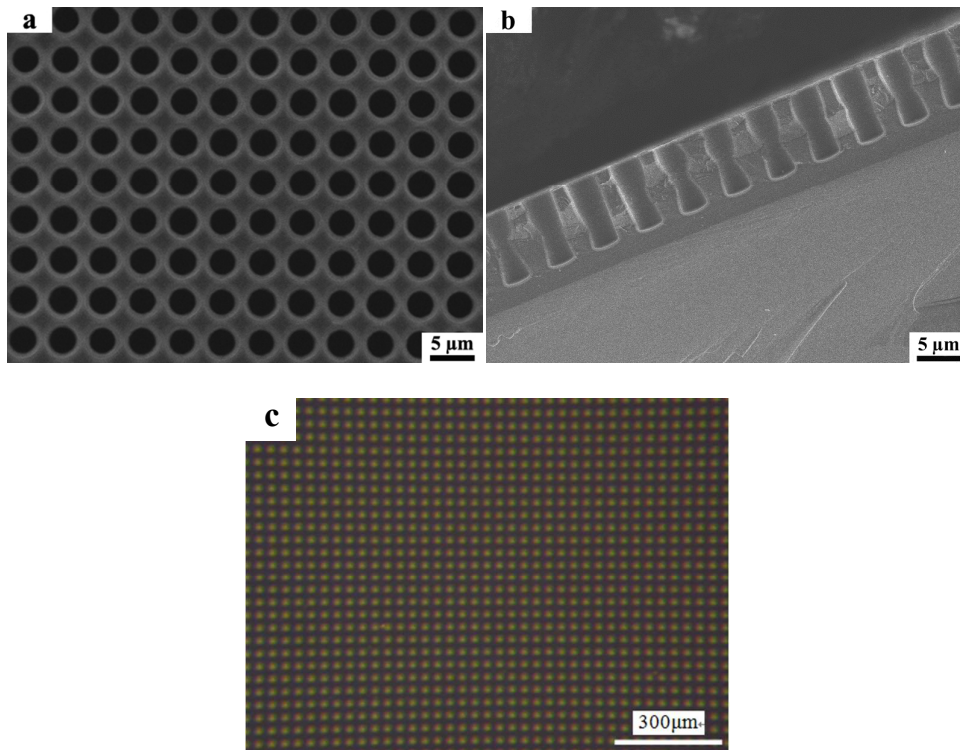
#### **S4. Measurements of ion exchange capability**

Both membranes were performed measurement of ion exchange capability. A slice of the pure Nafion membrane or the GO/Ag NPs doped Nafion membrane was put in the HCl solution (0.0374 mol/L), boiling for half an hour. Then, they were cleaned in deionized water, until solution color did not change under the addition of methyl orange. The samples were incubated in NaOH (0.0390 mol/L), and titrated with the HCl solution by using an indicator of tricyclohexyl tin hydride. Ion exchange capabilities were calculated with the equation:  $EW=(C_{NaOH}V_{NaOH}-C_{HCl}V_{HCl})/m$ .

#### **S5. Fabrication and characterizations of the Si negative template**

Both density and aspect-ratio (AR) influence the collapse of the setal micro-pillars. This is because capillary tension generated during dehydration causes adjacent setal

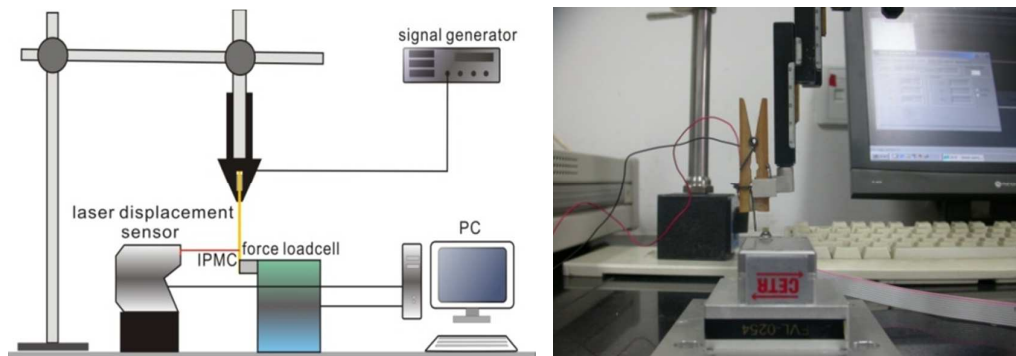
arrays to stick together. Previous literature demonstrates that, when AR of PDMS setal arrays is more than 3.5, setal arrays undergo lateral collapse.<sup>4</sup>To minimize collapse of the setal micro-pillars, we designed a mask for fabricating the negative pores(s-Figure 2a).Its pore diameter was 3  $\mu\text{m}$ , the pitch was 1.2  $\mu\text{m}$ , and the pore thickness was controlled around 10  $\mu\text{m}$ . Thus the AR was around 3.3, and less than the collapse limit of 3.5. The cross-sectional view (s-Figure 2b) exhibits a narrow, cylindrical structure of the pores with a thickness of around 10  $\mu\text{m}$ . Because the etching rate depends upon many factors such as Ar plasma concentration and reaction temperature, the pore radius and pore thickness slightly vary. S-Figure-2c recorded its optical photo with larger area.



**s-Figure 2.** SEM images (a: top view; and b: cross sectional view) and optical image (c) of the Si template

### S6. Setup for measurements of IPMC electromechanical performance

The blocking force of IPMC was detected by our customized system, including a signal generator, a signal amplifier, a Hall electric current sensor, and a 2-D force sensor (S-Figure-3 Left). The signal generator (SP1651, China Nanjing) has a multifunction data collection card (NI, 6024E), which can produce electrical signals with frequencies in the range of 0.1-100 Hz, voltages in the range of 0~5 V, and different waveforms (square, sinusoid and triangle). The signal amplifier is a power amplified chip (TI, OPA548) which provides power to actuate the IPMC sample. The Hall electric current sensor (TBC-A02) and the force sensor (CETR-UMT) were used to respectively collect the electric current through IPMC and the blocking force generated from IPMC. An IPMC slice with the dimension of 30×5 mm was actuated by a two-way square wave at the voltage of 1.0, 1.5, or 2.0V with a fixed frequency of 0.1Hz. It was placed on the force sensor for detecting the blocking force (S-Figure 3 Right). Before each actuation, IPMC was incubated in a LiOH (0.05mol/L) solution for water replenishment.

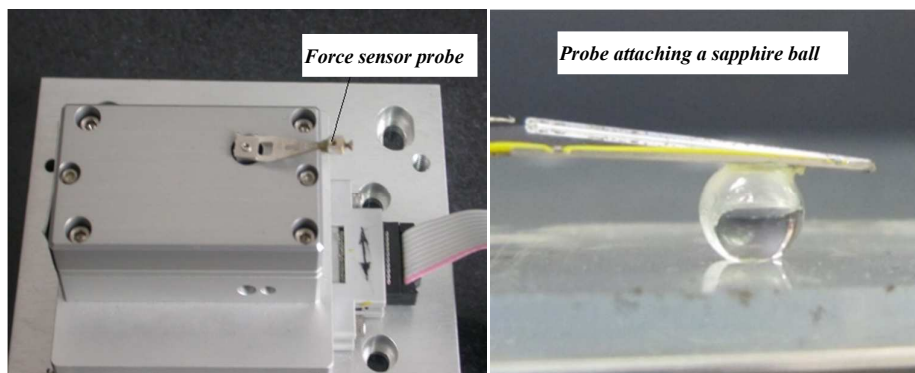


**S-Figure 3.** Illustration of the customized system setup for detecting blocking force and displacement (Left). Setup for detecting the blocking force by a force sensor from CETR (Right)

### **S7. Setup for adhesion performance measurements**

The former used 2-dimensional force sensor with a maximal force of 100 mN, and a sensitivity of 0.001 mN was employed to collect the adhesion data. The cantilever IPMC attaching the PMVS setal micropillars was suspended below the sapphire ball for testing the normal adhesion, and was placed on a planar surface under the sapphire ball for testing shear adhesion (friction). For comparing the detections of the blocking forces and adhesions, although the same force sensor was used, contact modes of transferring force were quite different. In the detection of the blocking force, a flat head tip was adhered on the probe's end to match the planar IPMC membrane (S-Figure-4 Left) and prevent IPMC twist. During the adhesion detection, a rigid sapphire ball with a radius of 1.87 mm was fixed at the end of force sensor acting as the upper mating ball, to ensure that the detected force was totally derived from adhesion (S-Figure-4 Right). Additionally, to ensure enough contact between the sapphire ball and the pillar-patterned IPMC surface, the blocking force of IPMC acted as normal preload, and was tailored by the applied voltage.





**S-Figure 4.** Force sensor adhering a flat head for detecting the blocking force (Left) and a sapphire ball for detecting the adhesions (Right).

#### REFERENCES

- (1) Guo, D. J.; Xiao, S. J.; Liu, H. B.; Xia, B.; Chao, J.; Pan, Y.; You, X. Z. Diffusion of Hydrosilanes from the Control Layer to the Vinylsilane-Rich Flow Membrane during the Fabrication of Microfluidic Chips. *Langmuir* **2005**, *21*, 10487-10491.
- (2) Li, D.; Mueller, M. B.; Gilje, S.; Kaner, R. B.; Wallace, G. G. Processable Aqueous Dispersions of Graphene Nanosheet. *Nat. nanotechnol.* **2008**, *3*, 101-105.
- (3) Hummers Jr. W. S.; Offeman, R. E. Preparation of Graphitic Oxide. *J. Am. Chem. Soc.* **1958**, *80*, 1339-1339.
- (4) Chandra, D.; Yang, S. Stability of High-AR Micropillar Arrays against Adhesive and Capillary Forces. *Acc. Chem. Res.* **2010**, *43*, 1080-1091.